J Herbmed Pharmacol. 2024; 13(2): 226-239.

http://www.herbmedpharmacol.com doi: 10.34172/jhp.2024.48154

Journal of Herbmed Pharmacology

# *In-silico* and biochemical analysis of ethyl acetate fraction of *Olax subscorpioidea* leaf on DMBA-induced cell proliferation in female rats

**Ayodeji Adebayo Adelegan[1*], Titilayo Omolara Johnson[2,3], Titilope Modupe Dokunmu[1,4], Emeka Eze Joshua Iweala[1,4]**

[1]Department of Biochemistry, College of Science and Technology, Covenant University, Ota, Ogun State, Nigeria
[2]Department of Biochemistry, Faculty of Basic Medical Science, College of Health Sciences, University of Jos, Jos, Nigeria
[3]Bioinformatics Unit, Jaris Computational Biology Centre, Jos, Nigeria
[4]Covenant Applied Informatics and Communication Africa Centre of Excellence, Covenant University, Ota, Ogun State, Nigeria

**ARTICLE INFO**

***Article Type:***
Original Article

***Article History:***
Received: 3 October 2023
Accepted: 18 December 2023

***Keywords:***
*Olax subscorpioidea,*
Bioinformatics,
Antioxidant,
Molecular dynamics,
Gas chromatography-mass spectrometry

**ABSTRACT**

**Introduction:** *Olax subscorpioidea* is a medicinal plant that Africans use to treat numerous ailments, including cancer. This research examines the antioxidant, anticancer, and *in-silico* properties of ethyl acetate fraction of *Olax subscorpioidea's* (OSEA) on 7,12-Dimethylbenz(α) anthracene (DMBA)-induced cell proliferation in female rats.

**Methods:** Forty female Sprague Dawley rats averaging 110 ± 20 g were induced proliferation with DMBA (80 mg/kg) and treated with ethyl acetate fraction (250 mg/kg BW) of *O. subscorpioidea* or tamoxifen (6.6 mg/kg BW) before and after induction. The trial lasted 22 weeks. *In-vivo* antioxidant parameters such as superoxide dismutase (SOD), malondialdehyde (MDA), and reduced glutathione (GSH) were examined. Likewise, carcinoma antigen marker (CA153), and DNA *methyltransferase* 3-like (DNMT3L) activity were measured. Gas chromatography-mass spectrometry (GC-MS) detected the bioactive compounds, and molecular docking studies predicted the mechanism of action of OSEA against DNA methyltransferase.

**Results:** Treatment with OSEA significantly increased the SOD activity, enhanced GSH levels, and lowered the levels of MDA, CA-153, and DNMT3L in DMBA-exposed rats. The GC-MS analysis of OSEA revealed the presence of 40 bioactive compounds. The molecular docking revealed that 4-cyclopentene-1,3-dione (-6.407 kcal/mol), 2-(2-hydroxyethylthio) (-4.926 kcal/mol) and 3,4,5,6-tetrahydrophthalic anhydride (-6.16 kcal/mol) had the lowest binding energies against DNMT1, DNMT3A, and DNMT3B, respectively. 2-(2-hydroxyethylthio) was the least toxic. The molecular dynamic simulation revealed that the interaction between DNMT3A and 2-(2-hydroxyethylthio) propionic was stable to an extent.

**Conclusion:** The *in-silico* and biochemical analysis of the ethyl acetate fraction of *O. subscorpioidea* showed that it can protect against lipid peroxidation and oxidative stress and may be a potent source of drug that serves as an effective therapeutic in the future.

*Implication for health policy/practice/research/medical education:*
Implications for Health Policy, Practice, Research, and Medical Education: This study demonstrates that the ethyl acetate fraction of *Olax subscorpioidea*'s (OSEA) possesses anticancer properties and might aid in developing natural-resource-based cancer treatments.

*Please cite this paper as:* Adelegan AA, Johnson TO, Dokunmu TM, Iweala EEJ. *In-silico* and biochemical analysis of ethyl acetate fraction of *Olax subscorpioidea* leaf on DMBA-induced cell proliferation in female rats. J Herbmed Pharmacol. 2024;13(2):226-239. doi: 10.34172/jhp.2024.48154.

## Introduction

Breast cancer is a prevalent global disease that unfortunately claims many lives. In an investigation in 2020, one in eight cancer diagnoses and 2.3 million new cases in both sexes were breast cancer, surpassing lung cancer as the most common malignancy (1). In 2020, it accounted for 25% of

***Corresponding author**: Ayodeji Adebayo Adelegan,
Email: ayodejiadelegan@gmail.com

all female cancer cases; it is growing globally, particularly in poorer nations (2). In 2020, 685 000 women died due to breast cancer (1); this amounted to 16% or 1 in every 6 cancer deaths in women (3). New breast cancer diagnoses are expected to increase to 3 million by 2040, and yearly deaths will approach 1 million. Thus, global efforts must increase to reduce this burden (3). Different subtypes have different prognoses and treatment responses (4,5). Breast cancer arises from genetic and epigenetic changes in normal cells that affect oncogene and tumour suppressor gene expression (6,7). Mutagenic chemicals, aging, radiation, ultraviolet light, oxygen radicals, chronic inflammation, and risk factors like smoking, overweight, obesity, alcohol addiction, and oestrogen exposure can damage genes and alter DNA methylation (6). DNA methylation, histone changes, and MiRNAs regulate gene expression in normal and diseased cells (8). DNA methyltransferase methylates DNA. Hypermethylation silences tumour suppressor genes, producing various illnesses, including cancer (9). DNA methylation is a promising cancer treatment target. Tumour development may be prevented by inhibiting DNA methyltransferase (9). Multiple investigations have shown anticancer plant species used in herbal medicine (10). Bioactive compounds in these plants have pharmacological effects, and their cancer-fighting mechanisms are currently being investigated. However, oxidative stress and antioxidants are important in cancer development and prevention, and many vegetables are good providers of antioxidants (11). Even though many medicinal plants have been used to treat cancer, many have yet to be fully researched. *Olax subscorpioidea*, a member of the Olacaceae, is one. This plant is common in Africa and has been used to address various health concerns, including asthma, inflammation, cough, infectious diseases, diabetes, hepatitis, and cancer (12). Popoola et al found that the herb may prevent and cure cancer (13). The aqueous leaf extract reduced iron-induced lipid peroxidation, abated free radicals and chelated and reduced iron (14). Notwithstanding the documented antioxidant and anticancer attributes of the plant, there is a dearth of information regarding the specific bioactive constituents that are accountable for its anticancer properties. In this study, we evaluated the *in-vivo* antioxidant and anticancer properties of the ethyl acetate fraction of *O. subscorpioidea* (OSEA), its interaction with the target protein (DNA methyltransferase) through molecular docking approach, and elucidated its pharmacokinetic properties through ADME prediction.

## Materials and Methods

### Experimental animals

A total of 40 adult female Sprague Dawley rats, aged 6-8 weeks and weighing an average of 110 ± 20 g, were used in the study. The animals were acclimatized for two weeks before commencement of the study at the covenant university animal handling facility in Ota, Ogun State, Nigeria. Throughout the study, animals were given a conventional mouse pellet meal and watered freely. Under controlled settings (12:12 hours light/dark cycles, 22 ± 3 °C ambient temperature, 50 ± 10% humidity), standard laboratory conditions were maintained.

### Collection and authentication of plant material

The fresh leaves of *O. subscorpioidea* were collected from the Gambari forest in southwest Nigeria in May 2021. The plant samples were validated by a botanist from the Forestry Research Institute of Nigeria (FRIN). Plant samples were submitted to the FRIN herbarium, and a voucher number of FHL 113038 was issued.

### Extraction of OSEA

Fresh leaves of *O. subscorpioidea* were air-dried in the laboratory for three weeks before pulverizing and storing them as powder. Petroleum ether was used to defat *O. subscorpioidea*. For 72 hours, it was cold macerated in 30:70 aqueous ethanol. At 50 °C, a rotary evaporator dried and concentrated the filtrate. Twenty grams of dry ethanol leaf extract of *O. subscorpioidea* was reconstituted in distilled water and extracted with hexane, ethyl acetate, butanol, and aqueous fraction (15).

### Gas chromatography-mass spectrometry (GC-MS) analysis

Ethyl acetate fraction of *O. subscorpioidea* (OSEA) was subjected to GC-MS analysis on Agilent 7890B gas chromatograph (Agilent, CA, USA) coupled with 5977B inert gas spectrometer with electron-impact source (Agilent, CA, USA) fitted with DB-1MS column (30 m × 0.32 mm × 0.25 µm). The carrier gas was helium, used at a constant flow of 1.5 mL/min at an initial nominal pressure of 3.2875 psi and an average velocity of 45.274 cm/s. Then, 0.5 µL of the samples were injected in splitless mode at an injection temperature of 300 °C purge flow to the split vent was 15 mL/min at 0.75 minutes with a total flow of 16.667 mL/min; the gas saver mode was switched off. The oven was initially programmed at 80 °C for 2 minutes and ramped at 20 °C/min to 200 °C for 4 minutes; after that it was ramped to 5 °C/min to 220 °C for 5 minutes then ramped at 10 °C/min to 230 °C for 12 minutes. The run time was 34 minutes. The mass spectrometer was operated in electron-impact ionization mode at 70 eV.

### *In vivo* studies

#### *Induction of mammary tumour in Sprague Dawley rats*

The method previously described by Zingue et al (16) was used to induce mammary tumours. Eighty (80 mg/kg) of DMBA was dissolved in 1 mL of olive oil and a single dose was administered orally to the entire experimental group aside from the normal control that received olive oil only. The rats were weighed and palpated weekly to observe any tumour development from the first day of induction to the

end of the experiment. The experiment lasted for 22 weeks. The rats that died during the experiment were recorded and all survivors were humanely sacrificed after treatment through the dislocation of the cervical vertebrae.

### *Grouping of animals and dosing*

Animals were separated into five groups with each group containing eight rats. The groups were classified as number I, II, III, IV, and V:

- Group I (Normal control group): The rats received intragastric olive oil three times a week throughout the trial.
- Group II (DMBA control group): The rats were induced with 80 mg/kg DMBA in olive oil and fed regular feed for the duration of the research.
- Group III (Tamoxifen group): The rats were given DMBA (80 mg/kg) and treated with 6.6 mg/kg oral tamoxifen thrice weekly. Treatment lasted one month.
- Group IV (Pre-OSEA group): The rats were pre-treated with oral administration of OSEA (250 mg/kg). Rats received thrice weekly from the start to the end of the experiment.
- Group V (OSEA-treated group): After 16 weeks of DMBA induction, rats were orally administered OSEA (250 mg/kg) thrice weekly. Treatment lasted one month.

### *Collection of blood and tissue samples*

Blood samples were collected from the surviving animals via the orbital vein and placed in bottles containing ethylenediaminetetraacetic acid (EDTA) and sample bottles. After that, the blood samples were centrifuged at 3000 × g for 10 minutes. The serum samples from the plain bottles were used for biochemical analysis (17). The livers were removed and then cleaned with a cold, saline solution, and kept at -30 °C to analyze oxidative stress and antioxidants (17).

### *Preparation of liver homogenate*

A quantity of 0.2 g of the liver from each group was minced and suspended in cold phosphate buffer (pH 7.4) with 0.024 M EDTA and homogenized on ice. The homogenate obtained was centrifuged for 10 minutes at 7000 rpm and the supernatant was used for the determination of superoxide dismutase (SOD), malondialdehyde (MDA), and reduced glutathione (GSH), respectively (17).

### *Oxidative stress evaluation*

### *Malondialdehyde*

The modified approach developed by Siddique et al identified lipid peroxidation (18). 15% trichloroacetic acid, 0.375% thiobarbituric acid, and 0.25 mol/L hydrochloric acid were diluted in 50 mL of distilled water. After combining 0.5 mL of sample with 1 mL of stock solution, the combination was boiled for 30 minutes in a boiling water bath. After 15 minutes of chilling and centrifuging at 2000 rpm, the clear supernatant of the sample was collected. At 535 nm, the sample absorbance was measured against a blank.

### *Superoxide dismutase*

The improved Markland technique detected and evaluated the SOD activity using pyrogallol autoxidation (19). One gram of material was combined with 9.0 mL distilled water for 10 minutes. After that, the mixture was put in a centrifuge tube with 10 mL of distilled water. The supernatant was obtained by centrifuging the mixture for 15 minutes at 4000 rpm. 2.35 mL of solution A (0.1 mol/L Tris-HCl buffer solution with 1 mmol/L EDTA at pH 8.2) and 2.00 mL distilled water were added to a 10 mL test tube to determine autoxidation. The test tube was vortexed after filling it with 0.15 mL of solution B (4.5 mmol/L pyrogallol in HCl). An aliquot of 325 nm absorbance was collected from a test tube. After 1 minute, another aliquot was collected. The absorbance difference between the aliquots was used to calculate pyrogallol autoxidation. A325 should be close to 0.060. The procedure described above was followed for the sample test. Before the application of Solution B, 200 µL of the sample was added. The sample solution was diluted to effectively reduce the autoxidation rate by 50%.

### *Reduced glutathione*

Reduced GSH was measured using the technique described by Prins and Loose (20). A 0.5 mL tissue homogenate sample was pipetted into a test tube containing 4 mL 0.08 N $H_2SO_4$ and thoroughly mixed. After 10 minutes at room temperature, the protein precipitation was performed with 0.5 mL of tungestate solution. The liquid was vigorously stirred for 5 minutes after the tube was sealed. To prevent a crust on the supernatant fluid during centrifugation, the solution was allowed to stand for a few minutes after the stopper was removed. The suspension was centrifuged at 860 G for 20 minutes. Two milliliters clear extract was pipetted to a container containing 2.5 mL tris buffer and 0.2 mL DNTB reagent. To make a reagent blank, the tissue homogenate was replaced with 2 mL of water. After 30-60 secs, the colour was appeared and the optical density was 412 nm.

### *Assay for CA153 serum tumour marker*

The levels of the rat mammary carcinoma antigen marker (CA-153) were assessed using an enzyme-linked immunosorbent assay (ELISA) kit manufactured by the Sunlong company in China. The ELISA kit is used for the quantification of CA-153 concentrations in rat serum, plasma, culture medium, or other biological fluids. The assay was done according to the manufacturer's instructions.

### *Assay for DNMT activity*

Rat DNA methyltransferase 3-like (DNMT3L) was measured according to the manufacturer (Sunlong) ELISA kit. This kit measures DNMT3L in rat serum, plasma, culture medium, or biological fluids.

### *In-silico* analysis of DNA methyltransferase inhibition potential

#### *Protein preparation*

The molecular docking study was conducted using Glide (Schrodinger Maestro 12.8), following the methodology published by Johnson et al (21). DNMT1, DNMT3A, and DNMT3B crystal structures were acquired from the Protein Data Bank (PDB) (http://www.rcsb.org/pdb/). The protein underwent preparation for the docking procedure utilizing the Glide protein preparation wizard panel to assign bond ordering, add hydrogen atoms, produce disulfide bonds, and substitute missing side chains and loops. OPLS3e and PROPKA were used to minimize and optimize protein structures after removing water molecules outside the 3.0 Å heteroatoms. S-adenosyl-L-homocysteine's co-crystallized location was used to create the receptor grid.

#### *Ligand preparation*

Using the Ligprep panel of Maestro 12.5 (Schrodinger Suite 2020-3), the compounds' structure data file (SDF) formats obtained from PubChem (https://pubchem.ncbi.nlm.nih.gov/) were converted to low-energy 3D structures with acceptable chiralities. A physiological pH of 7.2 ± 0.2 was used to establish ligand ionization states and calculate stereoisomer by constraining chiralities and varying others.

#### *Molecular docking*

Proteins and ligands were docked using the Glide-Ligand Docking panel in Maestro 12.5 (Schrodinger Suite 2020-3). The obtained ligands were docked into the active site of the target using extra precision docking. This involved employing a flexible ligand sampling technique, a vdW radius scaling factor of 0.80, and a partial charge cut-off of 0.15 for ligand atoms.

#### *Absorption, distribution, metabolism, excretion, and toxicity (ADMET) evaluation*

The ADMET properties of the test compounds were examined using integrated model predictions from the Swiss ADMET and PROTOX-II servers (22).

### Statistical analysis

The statistical package for social sciences (SPSS 23, IBM Corporation, Armonk, NY, USA) was used for statistical analysis, including one-way ANOVA and Duncan's test post-hoc multiple comparisons. At $P < 0.05$, the comparison was considered statistically significant. The data were displayed as mean ± SD of the experiment in triplicate.

## Results

### *In vivo* study

#### *The effect of OSEA on oxidative stress parameters in DMBA-induced proliferation in mammary rats*

Figure 1A reveals a 39.8% decrease in total SOD activity in rats treated with DMBA compared to the control group ($P<0.05$). The pre-OSEA 250 mg/kg group had a 27% increase in SOD activity. Both tamoxifen and OSEA-treated groups significantly increased the SOD activity by 46.5% and 44.9%, respectively.

Compared to the normal control group, the DMBA control group had a significant increase in MDA level, which was significantly reduced in the pre-OSEA and OSEA-treated groups (Figure 1B, $P < 0.05$).

Figure 2 shows that the reduced GSH level was significantly reduced in the DMBA control group compared to the normal control group, pre-OSEA, and OSEA-treated group.

#### *The effect of OSEA on serum tumour marker parameters in DMBA-induced proliferation in mammary rats*

Cancer antigen (CA-153) serum tumour marker activity

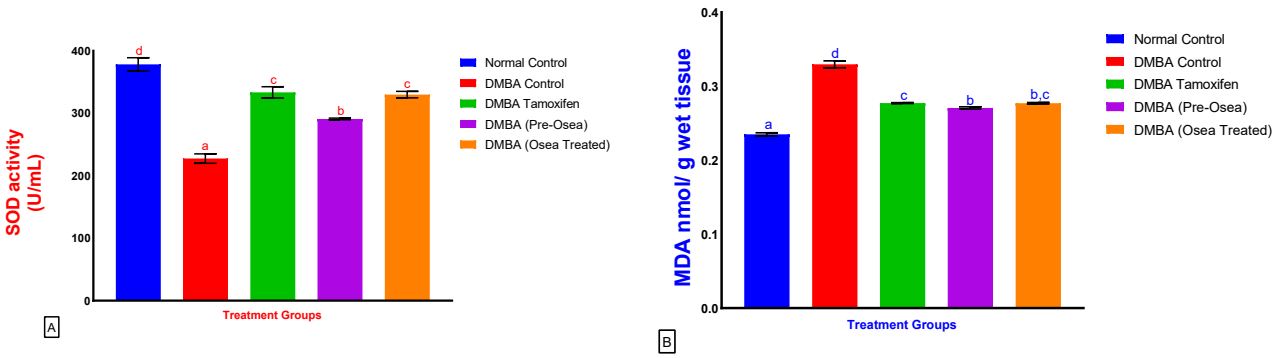


**Figure 1.** Effect of ethyl acetate fraction of *Olax subscorpioidea* (OSEA) on antioxidant parameters in 7,12-Dimethylbenz(α)anthracene (DMBA)-induced mammary rats. (A) Superoxide dismutase (SOD) and (B) Malondialdehyde (MDA). Groups with different letters in each figure show significant differences (Duncan test, $P < 0.05$).

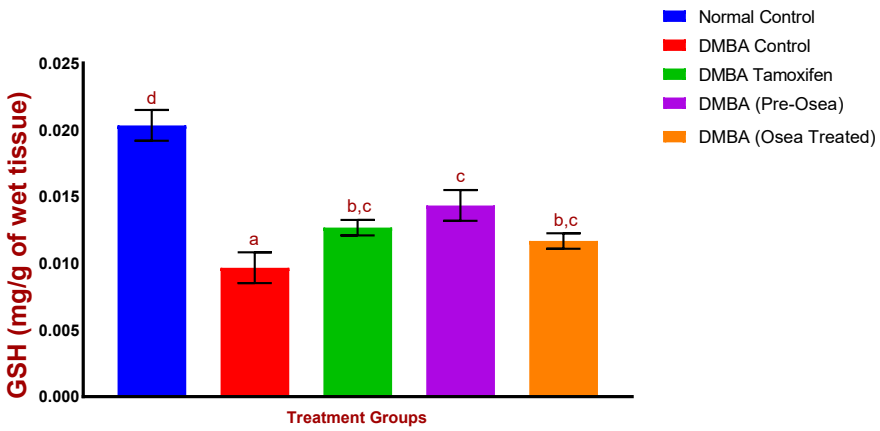


**Figure 2.** Effect of ethyl acetate fraction of *Olax subscorpioidea* (OSEA) on reduced glutathione (GSH) activity in 7,12-dimethylbenz(α)anthracene (DMBA)-induced mammary rats. Groups with different letters show significant differences (Duncan test, $P < 0.05$).

is shown in Figure 3. The DMBA group showed a significant increase ($P < 0.05$) in CA-153 levels compared to the control group. However, the rise was considerably reversed ($P < 0.05$) in the DMBA pre-OSEA and OSEA-treated groups.

### *The effect of OSEA on DNMT3L activity in DMBA-induced proliferation in mammary rats*

As seen in Figure 4, the DNMT3L activity in the DMBA control group was significantly higher than the control group. This increase was significantly reduced in the pre-OSEA and OSEA-treated groups.

### *GC-MS analysis*

The GC-MS analysis of OSEA revealed 40 compounds with specific retention time (RT), molecular formula (MF), molecular weight (MW), and concentration (% peak area) (Table 1). A previous GC-MS study carried out by Okoro et al (23) revealed the presence of seven major compounds in the ethanol leaf extract of *O. subscorpioidea* and twelve compounds in the ethanol stem bark extract of *O. subscorpioidea*. The compounds obtained from the GC-MS analysis of OSEA are classified under carboxylic acid, ketone, alcohol, and unsaturated fatty acid. The GC-MS phytochemical analyses relevant to this study were 4-cyclopentene-1,3-dione, 2-(2-hydroxyethylthio) propionic acid, and 3,4,5,6-tetrahydrophthalic anhydride.

### *In silico* analysis

### *Molecular docking*

The docking scores of the 10 top-scoring *O. subscorpioidea* compounds co-crystallized against DNMTs are shown in Table 2. 4-Cyclopentene-1,3-dione had the lowest binding energy against DNMT1 at -6.407 kcal/mol, followed by 1, 2-(2-hydroxyethylthio) propionic acid at -4.926 kcal/mol and 3,4,5,6-tetrahydrophthalic anhydride at -6.16 kcal/mol. Figure 5 displays the interaction between the co-crystallized ligand (Sinefungin) and 4-cyclopentene-1,3-dione with DNMT1. Sinefungin linked to DNMT1 via pi-pi stacking, salt bridge, and hydrogen bonds with PHE 1145, MET 1169, GLU 1168, ASN 1578, VAL 1580, LEU 1151, GLY 1150, GLY 1149, CYS 1148, and

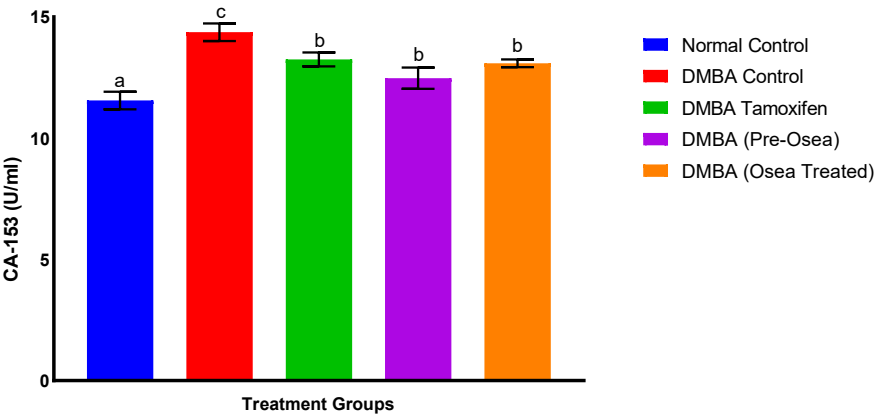


**Figure 3.** Effect of ethyl acetate fraction of *Olax subscorpioidea* (OSEA) on CA-153 activity in 7,12-dimethylbenz(α)anthracene (DMBA)-induced mammary rats. Groups with different letters show significant differences (Duncan test, $P < 0.05$).

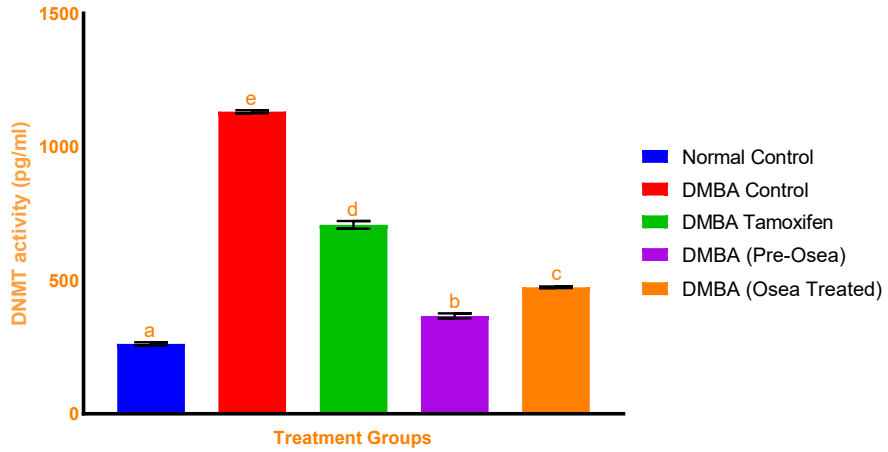


**Figure 4.** Effect of ethyl acetate fraction of *Olax subscorpioidea* (OSEA) on DNA methyltransferase (DNMT) activity in 7,12-Dimethylbenz(α)anthracene (DMBA)-induced mammary rats. Groups with different letters show significant differences (Duncan test, $P < 0.05$).

PHE 1145. Water molecules in the active site mediated hydrogen bonds. 4-Cyclopentene-1,3-dione formed hydrogen connections with CYS 1191 and MET 1169 and hydrophobic contacts with LEU 1247, CYS 1191, VAL 1144, PHE 1145, ILE 1167, TRP 1170, and PRO 1225. Figure 6 depicts the molecular interactions of 2-(2-Hydroxyethylthio) propionic acid and S-adenosyl-L-homocysteine (SAH) against DNMT3A. SAH bound to DNMT3A via two pi-pi stacking interactions with PHE 640, salt bridges with ARG 792 and GLU 756, hydrogen bonds with GLU 664, and one each with SER 708 and VAL 687. 2-(2-Hydroxyethylthio) propionic acid produced salt bridges and hydrogen bonds with ARG 891, SER 669, ILE 643, and ASP 641. SAH generated two pi-pi stacking contacts with PHE 581 and hydrogen bonds with GLU 605, VAL 628, ASP 627, PHE 581, ASP 582, ILE 584, THR 586, and TRP 834 with DNMT3B (Figure 7). DNMT3B interacted with 3,4,5,6-tetrahydrophthalic anhydride via hydrogen bonds with GLY 583, ILE 584, and THR 586 and hydrophobic contacts with LEU 580, PHE 581, ILE 584, and TRP 834.

### *ADMET property*

Table 3 shows ADMET properties for the three top-scoring compounds. The log *P* values of 4-cyclopentene-1,3-dione, 2-(2-hydroxyethylthio) propionic acid and

**Table 1.** Gas chromatography-mass spectrometry (GC-MS) identified compounds from ethyl acetate fraction of *Olax subscorpioidea* (OSEA)

| Compound number (#) | RT (min) | Area (Ab*s) | AH | Hit name | Chemical classification |
|---|---|---|---|---|---|
| 1 | 2.736 | 731054 | 799856 | 2-(2-Hydroxyethylthio) propionic acid | Carboxylic acid |
| 2 | 2.886 | 14887002 | 11470797 | 2-Butene, 2,3-dimethyl- | Ethene |
| 3 | 2.938 | 1738777 | 2231151 | 2-Pentanone, 3-methylene- | Ketone |
| 4 | 3.151 | 3640576 | 1804310 | Acetylacetone | Ketone |
| 5 | 3.28 | 10217894 | 5696498 | 3-Penten-2-one, 4-methyl- | Ketone |
| 6 | 3.446 | 3162417 | 864157 | Cyclotrisiloxane, hexamethyl- | Ester |
| 7 | 3.628 | 715905 | 700592 | 2-Cyclopenten-1-one | Ketone |
| 8 | 3.83 | 3110227 | 1987071 | Maleic anhydride | Unsaturated fatty acid |
| 9 | 3.976 | 6116083 | 2478549 | p-Xylene | Ethene |
| 10 | 4.079 | 811539 | 702144 | 4-Cyclopentene-1,3-dione | Ketone |
| 11 | 4.116 | 647253 | 677339 | Phenol | Alcohol |
| 12 | 4.157 | 4756982 | 3156563 | 1H-Imidazole, 1,4-dimethyl- | Aromatic heterocycles |
| 13 | 4.24 | 1321989 | 552762 | o-Xylene | Aromatic hydrocarbon |
| 14 | 4.474 | 548378 | 240745 | Butanoic acid, 4-hydroxy- | Hydroxy fatty acids |
| 15 | 4.598 | 450877 | 337858 | 3-Pentenal, 4-methyl- | Aldehydes |
| 16 | 4.832 | 482009 | 395165 | Cyclohexene, 1,6,6-trimethyl- | Sesquiterpenoids |
| 17 | 4.972 | 597902 | 343712 | Benzyl alcohol | Alcohol |
| 18 | 5.034 | 756430 | 457412 | 2-Cyclopenten-1-one, 2,3-dimethyl- | Cyclic ketones |

**Table 1.** Continued

| Compound number (#) | RT (min) | Area (Ab*s) | AH | Hit name | Chemical classification |
|---|---|---|---|---|---|
| 19 | 5.091 | 930542 | 644281 | 2-Cyclopenten-1-one, 3-methyl- | Cyclic ketones |
| 20 | 5.148 | 758630 | 483030 | Benzene, 1,2,3-trimethyl- | Aromatic hydrocarbon |
| 21 | 5.19 | 592295 | 371445 | Mesitylene | Aromatic hydrocarbon |
| 22 | 5.288 | 5473034 | 2370236 | Phosphonic acid, (p-hydroxyphenyl)- | Organophosphorus |
| 23 | 5.465 | 523924 | 276822 | Cyclohexene, 1-methyl-3-(formylmethyl)- | Unsaturated hydrocarbons |
| 24 | 5.517 | 2275486 | 767231 | Benzeneacetic acid, 4-methyl-. alpha.-[[(phenylmethylene)amino]methyl]-, methyl ester | Aromatic carboxylic acids |
| 25 | 5.818 | 885593 | 329378 | 3,4,5,6-Tetrahydrophthalic anhydride | Cyclic dicarboxylic acid anhydride |
| 26 | 6.243 | 814473 | 416077 | Phenol, 2-methyl- (O-Cresol) | Alcohol |
| 27 | 6.336 | 626432 | 433254 | Acetic acid, phenyl ester | Acetate ester |
| 28 | 6.414 | 1389458 | 941383 | Acetophenone | Aromatic ketones |
| 29 | 6.508 | 7682557 | 4301336 | Phenol, 3-methyl- (M-Cresol) | Alcohol |
| 30 | 6.892 | 2669130 | 1396802 | Benzofuran, 7-methyl- | Benzofurans |
| 31 | 6.964 | 917224 | 584674 | Benzofuran, 2-methyl- | Heterocyclic |
| 32 | 7.634 | 1133975 | 923640 | Acetic acid, 4-methylphenyl ester | Phenol esters |
| 33 | 7.68 | 2540057 | 1629412 | Phenol, 3,5-dimethyl- | Alcohol |
| 34 | 7.914 | 1166282 | 852012 | Naphthalene | Polycyclic aromatic hydrocarbon |
| 35 | 7.997 | 1027189 | 764972 | 2H-Pyran-2-one, 4,6-dimethyl- | Mesitene lactone |
| 36 | 8.085 | 1341903 | 951258 | 2,4-Dimethylfuran | Heteroaromatic |
| 37 | 8.189 | 1498955 | 1089974 | 1H-Benzimidazole, 5,6-dimethyl- | Benzimidazoles |
| 38 | 8.282 | 2383158 | 1044443 | 1H-Benzimidazole, 2-ethyl- | Heterocyclic |
| 39 | 8.396 | 922789 | 456823 | 4H-Pyran-4-one, 2,6-dimethyl- | Pyrans |
| 40 | 9.476 | 676788 | 532871 | 2,5,6-Trimethylbenzimidazole | Benzimidazoles |

AH: Absolute height, RT: Retention time.

**Table 2.** Docking scores (kcal/mol) of the ten top-scoring bioactive compounds of ethyl acetate fraction of *Olax subscorpioidea* (OSEA) against DNMT1, DNMT3A, and DNMT3B

| DNMT1 (PDP ID: 3SWR) | | DNMT3A (PDP ID: 4U7P) | | DNMT3B (PDB ID:6KDL) | |
|---|---|---|---|---|---|
| **Compound name** | **Docking score: ΔG Energy (kcal/mol)** | **Compound name** | **Docking score: ΔG Energy (kcal/mol)** | **Compound name** | **Docking score: ΔG Energy (kcal/mol)** |
| Sinefungin* | -8.253 | S-adenosyl-L-homocysteine (SAH)* | -8.639 | SAH* | -8.456 |
| 4-Cyclopentene-1,3-Dione | -6.407 | 2-(2-Hydroxyethylthio)propionic acid | -4.926 | 3,4,5,6-tetrahydrophthalic anhydride | -6.16 |
| Acetylacetone | -5.842 | 5,6-Dimethylbenzimidazole | -4.84 | Phosphonic acid, (p-hydroxyphenyl)- | -6.116 |
| Maleic anhydride | -5.564 | Acetophenone | -4.779 | O-Cresol | -5.268 |
| M-Cresol | -5.446 | Acetylacetone | -4.769 | 1H-Benzimidazole, 5,6-dimethyl- | -5.179 |
| O-Cresol | -5.428 | 3,4,5,6-Tetrahydrophthalic anhydride | -4.635 | Phenol | -4.796 |
| Phenol | -5.309 | 4-Cyclopentene-1,3-dione | -4.472 | Benzyl alcohol | -4.698 |
| Acetophenone | -5.134 | Phosphonic acid, (p-hydroxyphenyl)- | -4.463 | Butanoic acid, 4-hydroxy- | -4.489 |
| 7-methylbenzofuran | -4.918 | O-Cresol | -4.199 | 4H-Pyran-4-one, 2,6-dimethyl- | -4.298 |
| 2-Cyclopenten-1-one, 2,3-dimethyl- | -4.755 | Maleic anhydride | -4.194 | Phenol, 3,5-dimethyl- | -4.031 |
| 4H-Pyran-4-one, 2,6-dimethyl- | -4.628 | 2-Cyclopenten-1-one, 2,3-dimethyl- | -4.104 | 2H-Pyran-2-one, 4,6-dimethyl- | -4.027 |

* Co-crystallized ligand; DNMT: DNA methyltransferase.

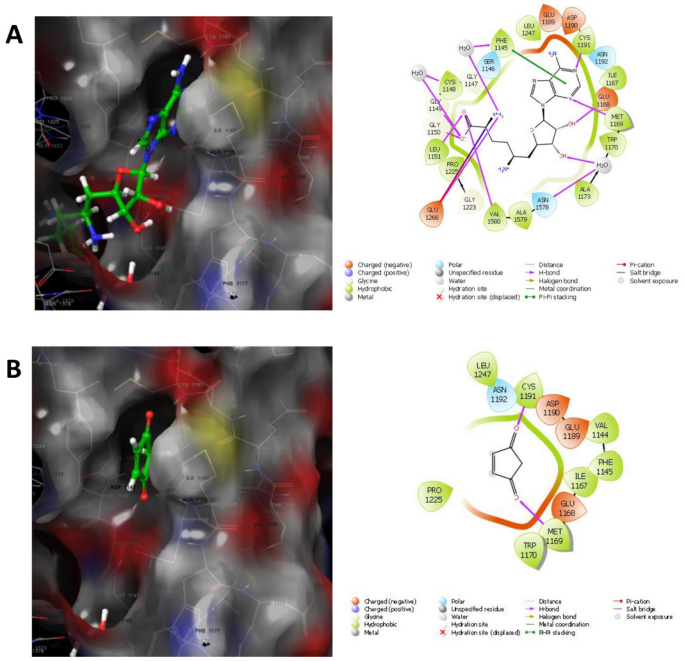


**Figure 5.** 3D (left) and 2D (right) views of the molecular interactions of A: Sinefungin and B: 4-Cyclopentene-1,3-Dione with DNA methyltransferase 1 (DNMT1).

3,4,5,6-tetrahydrophthalic anhydride were 0.30, 0.32, and 1.38, receptively (All are water soluble). The three compounds obeyed Lipinski's rule; they all possessed high gastrointestinal (GI) tract absorption, and their bioavailability scores were 0.55, 0.56, and 0.55, respectively. The $LD_{50}$ values of the compounds were 3000, 5700, and 700 mg/kg, respectively. The compounds belong to the toxicity classes 5, 6, and 4, with 4-cyclopentene-1,3-dione

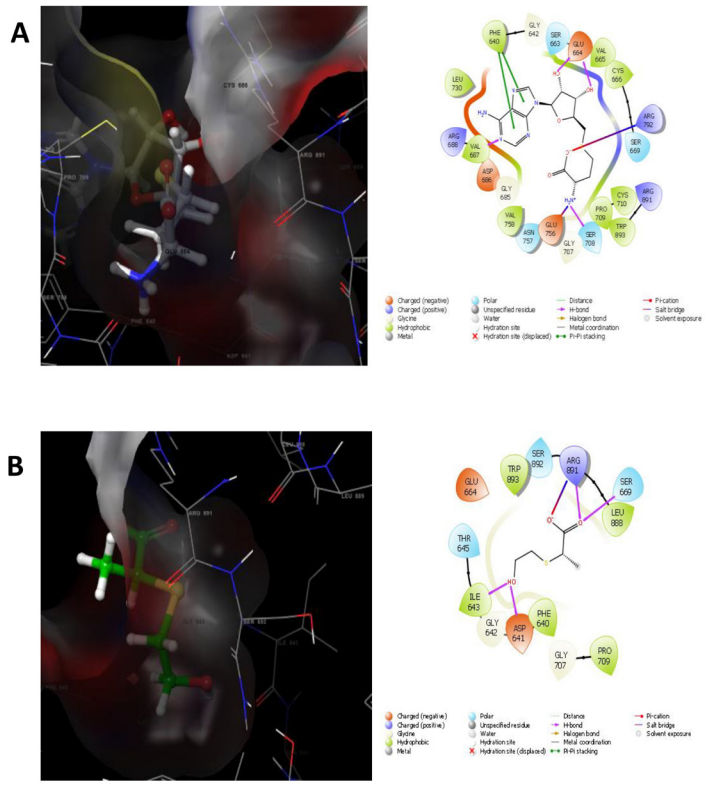


**Figure 6.** 3D (left) and 2D (right) views of the molecular interactions of A: S-adenosyl-L-homocysteine and B: 2-(2-Hydroxyethylthio) propionic acid with DNA methyltransferase 3A (DNMT3A).

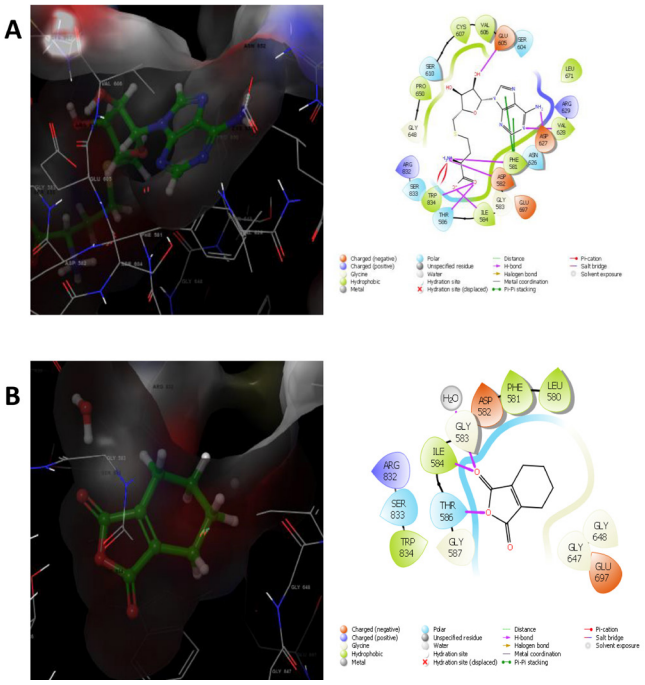


**Figure 7.** 3D (left) and 2D (right) views of the molecular interactions of A: S-adenosyl-L-homocysteine and B: 3,4,5,6-tetrahydrophthalic anhydride with DNA methyltransferase 3B (DNMT3B).

having the potential for carcinogenicity.

### *Molecular dynamics simulation*

The backbone atom of DNMT3A had a root mean square deviation (RMSD) value of 2.483 Å for the first 1 ns, 3.6 Å at 45 ns, and consistent variations around this value throughout the 100 ns simulation. Figure 8 shows that the ligand's RMSD value increased from 0.1 Å at 1 ns to 3.6 Å at 60 ns, eventually becoming unstable and decreasing throughout the simulation. DNMT3A residues interacted with 2-(2-hydroxyethylthio) propionic acid during MD simulation. As shown in Figure 9, the ligand properties remained unstable throughout the simulation, as indicated by the RMSD, radius of gyration (rGyr), intramolecular hydrogen bonds (intraHB), molecular surface area (MolSA), solvent accessible surface area (SASA), and polar surface area (PSA). As demonstrated in Figure 10, ARG 891 had two hydrogen bond interactions with GLU 891 for 41% and 42%. These interactions appear to be relatively stable.

## Discussion

Many medicinal plants show potential in fighting cancer, but few have been fully researched. One example is *O. subscorpioidea* a member of Olacaceae (12). Although the plant is known for its antioxidant and anticancer effects, its bioactive components and mechanisms of action are unknown. This study investigated OSEA for *in-vivo* anticancer activity in rats and identified the active components *in-silico*.

In the *in vivo* study, total SOD activity and reduced GSH to oxidized GSH (GSSG) were significantly reduced in the DMBA group. Also, the MDA level was significantly increased in the DMBA group. Following treatment with tamoxifen (standard anticancer drug), and OSEA, the SOD activity increased significantly. The MDA level was reduced and there was an increase in the level of GSH. SOD enzymes convert the superoxide anion ($O_2^-$) radical into hydrogen peroxide ($H_2O_2$). This hydrogen peroxide is then broken down into water and oxygen by catalase and glutathione peroxidase. This process effectively prevents oxidative damage (22). However, carcinogen exposure increases free radical generation, which decreases antioxidant defense system components and increases oxidative stress (22), a major element in breast cancer etiology. This explains the reduced SOD activity observed in the DMBA-exposed rats, and the ability of OSEA to increase SOD activity is suggestive of its antioxidant potential. The extract increased the level of GSH, indicating its antioxidant properties. GSH, the most abundant thiol in mammalian cells, neutralizes reactive oxygen species (24). The GSH-to-GSSG ratio measures cellular oxidative stress (25). A higher ratio indicates less stress. DMBA-exposed rats treated with OSEA had considerably lower lipid peroxidation, indicating less oxidative damage. Lipid peroxidation causes MDA production, a significant secondary hallmark of oxidative damage (26). Hence, the findings of this investigation support the fact that therapeutic intervention aimed at modulating SOD activity, GSH levels, and lipid peroxide

**Table 3.** ADMET (Absorption, distribution, metabolism, excretion, and toxicity properties of the three top-scoring compounds of the ethyl acetate fraction of Olax subscorpioidea (OSEA)

| ADMET property | Parameter | A | B | C |
|---|---|---|---|---|
| Lipophilicity | Consensus Log P | 0.30 | 0.32 | 1.38 |
| Water solubility | Silicos-IT Class | Soluble | Soluble | Soluble |
| | Lipinski violations | 0 | 0 | 0 |
| Pharmacokinetics | GI absorption | High | High | High |
| | Bioavailability Score | 0.55 | 0.56 | 0.55 |
| **Toxicity profile** | Predicted LD50 (mg/kg) | 3000 | 5700 | 700 |
| | Toxicity class | 5 | 6 | 4 |
| | Hepatotoxicity | - | - | - |
| | Mutagenicity | - | - | - |
| | Carcinogenicity | + | - | - |
| | Immunotoxicity | - | - | - |
| | Cytotoxicity | - | - | - |
| | AhR | - | - | - |
| | AR | - | - | - |
| | AR-LBD | - | - | - |
| | Aromatase | - | - | - |
| | Erα | - | - | - |
| | ER-LBD | - | - | - |
| | PPAR-γ | - | - | - |
| | Nrf2/ARE | - | - | - |
| | HSE | - | - | - |
| | MMP | - | - | - |
| | p53 | - | - | - |
| | ATAD5 | - | - | - |

(MDA) production might be beneficial in the management and prevention of breast cancer. This is supported by the impact of OSEA on the levels of blood tumour markers and the activity of DNMT3L in rats exposed to DMBA.

The serum tumour marker (CA15-3) and DNA methyltransferase activity of DMBA-exposed rats treated with OSEA were considerably lower than those in the untreated groups. Breast cancer patients' serum CA15-3 levels are evaluated regularly throughout therapy. The apical membrane of epithelial ducts and acinic breast cells secrete CA15-3 into breast milk. Cancer metastases may be detected by blood CA15-3 levels. CA15-3 enters the bloodstream during cancer due to altered breast shape (27,28). DMBA-exposed rats had higher serum CA15-3 levels, explaining this study's findings. DNA methyltransferase, another breast cancer indication, methylates cytosine at the 5-position. The most common epigenetic change in animals is DNA methylation. In accordance with the results obtained in this study, the levels of DNMTs, including that of DNMT3L, are frequently elevated in many kinds of cancerous tissues and cell lines (29). Thus, *O. subscorpioidea* considerably lowers blood levels of these markers, supporting its anticancer potential.

GC-MS and *in-silico* analysis of OSEA were conducted to identify its active ingredients on account of its promising anticancer activity. The GC-MS analysis identified 40 compounds, which were investigated for their abilities to inhibit the anti-cancer therapeutic targets DNMT1, DNMT3A, and DNMT3B using molecular docking and ADMET analysis. Molecular docking showed that chemicals had different protein target binding affinities. 2-(2-Hydroxyethylthio) propionic acid scored the highest against DNMT3A with -4.926 kcal/mol, while 3,4,5,6-tetrahydrophthalic anhydride scored the highest against DNMT3B with -6.16 kcal/mol. Top-scoring compounds occupied the same binding site as co-crystallized ligands and interacted with DNMT inhibitor-targeted active site amino acid residues. Many cancer tissues and cell lines have high DNMT levels, and inhibiting it, using active site amino acids residues, reduces tumour growth. DNMT1, DNMT3A, DNMT3B, and the methyltransferase-like protein (DNMT3L) are responsible for DNA (cytosine-5) methylation in animals.

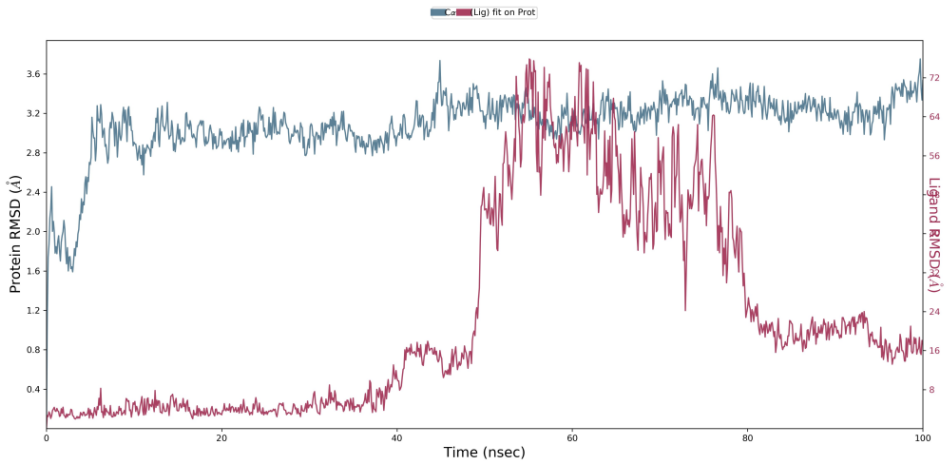


**Figure 8.** The protein and ligand Root Mean Square Deviation (RMSD) with respect to the reference frame (at time T = 0) during 100ns molecular dynamic (MD) simulation. Left Y-axis: RMSD evolution of DNMT3A; right Y-axis: RMSD for 2-(2-hydroxyethylthio) propionic acid.

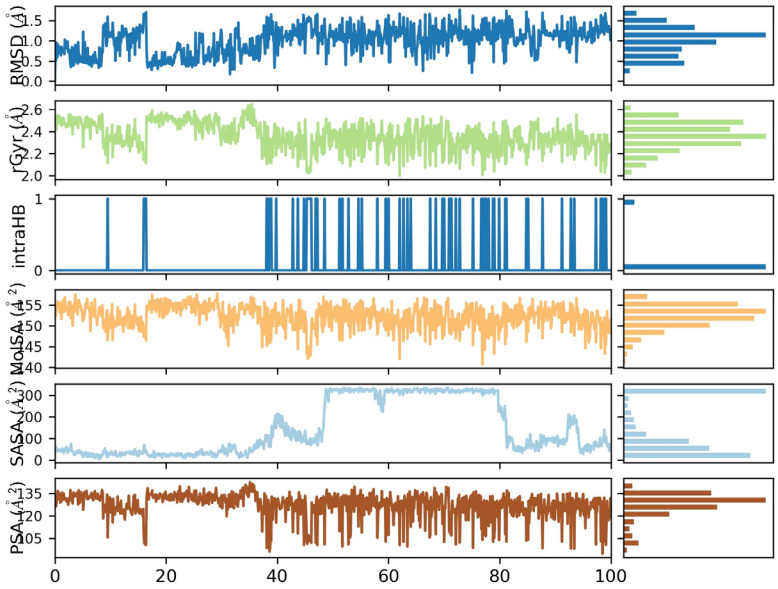


**Figure 9.** The ligand properties comprising of Root Mean Square Deviation (RMSD), radius of Gyration (rGyr), intramolecular hydrogen bonds (intraHB), molecular surface area (MolSA), solvent accessible surface area (SASA), and polar surface area (PSA).

DNMT1 enzymes largely maintain DNA methylation patterns. As the major enzyme that copies methylation patterns after DNA replication, DNMT1 is called maintenance methyltransferase (30). DNMT3A and DNMT3B genes encode two related proteins that are de novo methyltransferases (29,31). Inhibition of DNMT1, DNMT3A, and DNMT3B increases tumour suppressor gene expression and reduces tumour growth. The three highest-scoring *O. subscorpioidea* in this investigation showed binding affinities and molecular interactions that indicate they might be used as anticancer medicines. However, the structural features of the compounds could be further modified through lead optimization to improve the binding affinities, which are slightly lower than those of the standard inhibitors (co-crystallized ligand). This could also help minimize some toxic potential as revealed by the ADMET analysis.

ADMET study assesses whether a chemical can be safely absorbed, transported, metabolized, and eliminated (21).

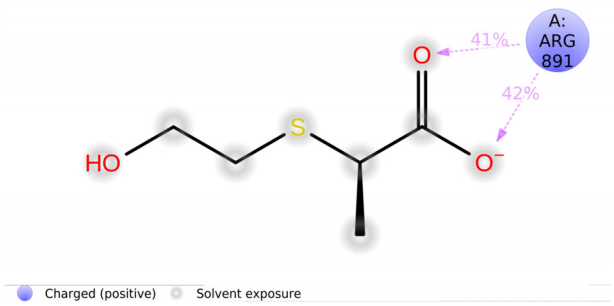


**Figure 10.** An illustration of how the ligand atoms interact with the protein sites displaying interactions that happen more than 30% of the time in the chosen route.

Drug ADMET depends on lipophilicity and water solubility. Oral medications must be lipophilic and hydrophilic to enter circulation (21). The three *O. subscorpioidea* compounds with log *P* values between 0.30 and 1.38 were suitable for target cell absorption, distribution, and protein access. This is supported by drug-like substances. Drug-likeness analysis employing rule-based approaches like the Lipinski filter estimates oral bioavailability qualitatively (32). The Lipinski filter requires oral medications to have a log P of less than 5, a molecular weight of less than 500 g/mol, and a maximum of 5 hydrogen bond donors and 10 acceptors (33). A chemical can't be orally active if it fails to meet more than one of the requirements. The chosen *O. subscorpioidea* compounds have no Lipinski violation and may be orally accessible. These findings match the drugs' expected pharmacokinetics, which exhibited high GI absorption and bioavailability scores between 0.55 and 0.56. The chemicals may be orally bioavailable with a 55% and 56% likelihood of at least 10% oral bioavailability in rats or detectable human colon cancer (Caco-2) permeability (32). Despite their excellent drug-likeness and pharmacokinetics, the chemicals' toxicity profile will decide their anti-cancer efficacy. 4-Cyclopentene-1,3-dione, 2-(2-hydroxyethylthio) propionic acid and 3,4,5,6-tetrahydrophthalic anhydride have responsive $LD_{50}$ values of 3000 mg/kg (class 5), 5700 mg/kg (class 6), and 700 mg/kg. However, 4-cyclopentene-1,3-dione may be carcinogenic, so it should be used with care. This negative impact may be reduced via lead optimization.

Due to its low toxicity, 2-hydroxyethylthiopropionic acid was chosen as the compound to be simulated using molecular dynamics. Understanding the nature and breadth of protein-ligand and intermolecular interactions

requires the use of molecular dynamics modeling. By examining deviations and variations, MD simulation may show the ligand's dynamic behavior and stability versus the protein (34,35). RMSD was used to calculate protein backbone deviation during simulation (36). As shown in Figure 8, the initial change in the RMSD values of the protein and ligand is the result of a rise in system temperature (34). Nonetheless, this complex destabilizes after 100 ns. The RMSD values remained unstable until the conclusion of the simulation, following an initial increase. This indicates that the complex formed by DNMT3A in conjunction with 2-(2-hydroxyethylthio)propionic acid is somewhat unstable.

Additional ligand characteristics during simulation show complex stability. Ligand "extendedness" and fundamental moment of inertia are measured by the radius of gyration. Internal hydrogen bonding of ligand molecules is quantified. The Molar Surface Area is calculated from the compound's surface using a probe radius of 1.4. This number also indicates the van der Waals surface area. The water contact area is measured by SASA. Nitrogen and oxygen dominate the compound's solvent-accessible PSA (Schrodinger Release, EUR 2018). Each of these attributes changed within a range throughout the simulation, indicating that the protein-ligand combination is stable. During simulation, protein-ligand interactions should be varied and consistent. The chemical remained in contact with the active site residues ARG 891 throughout the simulation, via hydrogen bonds and water bridges. Complex relationships varied during the trial. ARG 891 sustained two hydrogen bond connections with the ligand for 41% and 42% of simulations. Hydrogen bonds between protein and ligand stabilize the complex (31). 2-(2-Hydroxyethylthio)propionic acid's DNMT3A-inhibiting and anti-cancer activities depend on stability. Simulations indicate that DNMT3A's interaction with 2-(2-hydroxyethylthio) propionic acid is stable to an extent. Therefore, compound optimization is advised.

## Conclusion

The ethyl acetate fraction of *O. subscorpioidea* showed remarkable antioxidant and anticancer properties in this study. The GC-MS analysis of the extract revealed the presence of many bioactive chemicals that possess the capability to inhibit the DNA methyltransferase enzyme. To enhance the reliability of the findings, a computational study was conducted, including Admet, toxicological analysis, molecular docking, and molecular dynamics modeling, which further validated the plant's anticancer characteristics.

### Acknowledgment

The authors are grateful to the Jaris Computational Biology Centre (Jaris Research) where the computational studies were carried out.

### Authors' contributions

**Conceptualization:** Ayodeji Adebayo Adelegan, Titilope Modupe Dokunmu, and Emeka Eze Joshua Iweala.
**Data curation:** Ayodeji Adebayo Adelegan and Titilayo Omolara Johnson.
**Formal analysis:** Ayodeji Adebayo Adelegan and Titilayo Omolara Johnson.
**Investigation:** Ayodeji Adebayo Adelegan, Titilope Modupe Dokunmu, and Emeka Eze Joshua Iweala.
**Methodology:** Ayodeji Adebayo Adelegan, Titilayo Omolara Johnson, Titilope Modupe Dokunmu, and Emeka Eze Joshua Iweala.
**Project administration:** Emeka Eze Joshua Iweala and Titilope Modupe Dokunmu.
**Resources:** Emeka Eze Joshua Iweala, Ayodeji Adebayo Adelegan and Titilayo Omolara Johnson.
**Software:** Titilayo Omolara Johnson.
**Supervision:** Emeka Eze Joshua Iweala and Titilope Modupe Dokunmu.
**Validation:** Ayodeji Adebayo Adelegan, Titilayo Omolara Johnson, Titilope Modupe Dokunmu, and Emeka Eze Joshua Iweala.
**Visualization:** Ayodeji Adebayo Adelegan and Titilayo Omolara Johnson.
**Writing-original draft:** Ayodeji Adebayo Adelegan, Titilayo Omolara Johnson, Titilope Modupe Dokunmu, and Emeka Eze Joshua Iweala.
**Writing-review & editing:** Ayodeji Adebayo Adelegan, Titilayo Omolara Johnson, Titilope Modupe Dokunmu, and Emeka Eze Joshua Iweala .

### Conflict of interests

The authors declare that they have no known competing financial interests or personal relationships that could have appeared to influence the work reported in this paper.

### Ethical considerations

The National Institute of Health (NIH) Office of Animal Care and Use (2016) criteria were followed for laboratory animal care and experimentation. Before beginning the animal study, Covenant University's Health Research Ethics Committee granted ethical permission and provided a protocol number (CHREC /162/2022).

### References

1. Sung H, Ferlay J, Siegel RL, Laversanne M, Soerjomataram I, Jemal A, et al. Global cancer statistics 2020: GLOBOCAN estimates of incidence and mortality worldwide for 36 cancers in 185 countries. CA Cancer J Clin. 2021;71(3):209-49. doi: 10.3322/caac.21660.
2. Heer E, Harper A, Escandor N, Sung H, McCormack V, Fidler-Benaoudia MM. Global burden and trends in premenopausal and postmenopausal breast cancer: a population-based study. Lancet Glob Health. 2020;8(8):e1027-37. doi: 10.1016/s2214-109x(20)30215-1.
3. Arnold M, Morgan E, Rumgay H, Mafra A, Singh D, Laversanne M, et al. Current and future burden of breast cancer: global statistics for 2020 and 2040. Breast. 2022;66:15-23. doi: 10.1016/j.breast.2022.08.010.

4. Waks AG, Winer EP. Breast cancer treatment: a review. JAMA. 2019;321(3):288-300. doi: 10.1001/jama.2018.19323.
5. Fragomeni SM, Sciallis A, Jeruss JS. Molecular subtypes and local-regional control of breast cancer. Surg Oncol Clin N Am. 2018;27(1):95-120. doi: 10.1016/j.soc.2017.08.005.
6. Takeshima H, Ushijima T. Accumulation of genetic and epigenetic alterations in normal cells and cancer risk. NPJ Precis Oncol. 2019;3:7. doi: 10.1038/s41698-019-0079-0.
7. Carlos-Reyes Á, López-González JS, Meneses-Flores M, Gallardo-Rincón D, Ruíz-García E, Marchat LA, et al. Dietary compounds as epigenetic modulating agents in cancer. Front Genet. 2019;10:79. doi: 10.3389/fgene.2019.00079.
8. De Almeida BP, Apolónio JD, Binnie A, Castelo-Branco P. Roadmap of DNA methylation in breast cancer identifies novel prognostic biomarkers. BMC Cancer. 2019;19(1):219. doi: 10.1186/s12885-019-5403-0.
9. Mirza S, Sharma G, Parshad R, Gupta SD, Pandya P, Ralhan R. Expression of DNA methyltransferases in breast cancer patients and to analyze the effect of natural compounds on DNA methyltransferases and associated proteins. J Breast Cancer. 2013;16(1):23-31. doi: 10.4048/jbc.2013.16.1.23.
10. Desai AG, Qazi GN, Ganju RK, El-Tamer M, Singh J, Saxena AK, et al. Medicinal plants and cancer chemoprevention. Curr Drug Metab. 2008;9(7):581-91. doi: 10.2174/138920008785821657.
11. Sharifi-Rad M, Anil Kumar NV, Zucca P, Varoni EM, Dini L, Panzarini E, et al. Lifestyle, oxidative stress, and antioxidants: back and forth in the pathophysiology of chronic diseases. Front Physiol. 2020;11:694. doi: 10.3389/fphys.2020.00694.
12. Ahmad MH, Jatau AI, Alshargi OY, Julde SaM, Mohammed M, Muhammad S, et al. Ethnopharmacological uses, phytochemistry, pharmacology, and toxicology of *Olax subscorpioidea* Oliv (Olacaceae): a review. Futur J Pharm Sci. 2021;7(1):115. doi: 10.1186/s43094-021-00264-w.
13. Popoola TD, Awodele O, Babawale F, Oguns O, Onabanjo O, Ibanga I, et al. Antioxidative, antimitotic, and DNA-damaging activities of *Garcinia kola* stem bark, *Uvaria chamae* root, and *Olax subscorpioidea* root used in the ethnotherapy of cancers. J Basic Clin Physiol Pharmacol. 2019;31(3):20190073. doi: 10.1515/jbcpp-2019-0073.
14. Saliu JA, Olabiyi AA. Aqueous extract of *Securidaca longipendunculata* Oliv. and *Olax subscropioidea* inhibits key enzymes (acetylcholinesterase and butyrylcholinesterase) linked with Alzheimer's disease in vitro. Pharm Biol. 2017;55(1):252-7. doi: 10.1080/13880209.2016.1258426.
15. Adelegan AA, Dokunmu TM, Iweala EE. In-vitro antioxidant activity and cytotoxic effect of ethanol leaf extract and fractions of *Olax subscorpioidea* Oliv. (Olacaceae). Trop J Nat Prod Res. 2023;7(8):3806-12. doi: 10.26538/tjnpr/v7i8.35.
16. Zingue S, Njuh AN, Tueche AB, Tamsa J, Tchoupang EN, Kakene SD, et al. In vitro cytotoxicity and in vivo antimammary tumor effects of the hydroethanolic extract of *Acacia seyal* (Mimosaceae) stem bark. Biomed Res Int. 2018;2018:2024602. doi: 10.1155/2018/2024602.
17. Iweala EE, Evbakhavbokun WO, Maduagwu EN. Antioxidant and hepatoprotective effect of *Cajanus cajan* in N-nitrosodiethylamine-induced liver damage. Sci Pharm. 2019;87(3):24. doi: 10.3390/scipharm87030024.
18. Siddique YH, Ara G, Afzal M. Estimation of lipid peroxidation induced by hydrogen peroxide in cultured human lymphocytes. Dose Response. 2012;10(1):1-10. doi: 10.2203/dose-response.10-002.Siddique.
19. Li X. Improved pyrogallol autoxidation method: a reliable and cheap superoxide-scavenging assay suitable for all antioxidants. J Agric Food Chem. 2012;60(25):6418-24. doi: 10.1021/jf204970r.
20. Prins GK, Loose JA. Biochemical methods in red blood cell genetics. In: Glutathione. London: Academic Press; 1969. p. 126-9.
21. Johnson TO, Adegboyega AE, Iwaloye O, Eseola OA, Plass W, Afolabi B, et al. Computational study of the therapeutic potentials of a new series of imidazole derivatives against SARS-CoV-2. J Pharmacol Sci. 2021;147(1):62-71. doi: 10.1016/j.jphs.2021.05.004.
22. Johnson TO, Odoh KD, Nwonuma CO, Akinsanmi AO, Adegboyega AE. Biochemical evaluation and molecular docking assessment of the anti-inflammatory potential of *Phyllanthus nivosus* leaf against ulcerative colitis. Heliyon. 2020;6(5):e03893. doi: 10.1016/j.heliyon.2020.e03893.
23. Okoro CO, Aloke C, Ibiam UA, Obasi NA, Orji OU, Ogbonnia EC, et al. Studies on ethanol extracts of *Olax subscorpioidea* against carbon tetrachloride-induced hepatotoxicity in rats. Pak J Biol Sci. 2021;24(6):724-32. doi: 10.3923/pjbs.2021.724.732.
24. Iskusnykh IY, Zakharova AA, Pathak D. Glutathione in brain disorders and aging. Molecules. 2022;27(1):324. doi: 10.3390/molecules27010324.
25. Lu SC. Glutathione synthesis. Biochim Biophys Acta. 2013;1830(5):3143-53. doi: 10.1016/j.bbagen.2012.09.008.
26. Wang Z, Li S, Cao Y, Tian X, Zeng R, Liao DF, et al. Oxidative stress and carbonyl lesions in ulcerative colitis and associated colorectal cancer. Oxid Med Cell Longev. 2016;2016:9875298. doi: 10.1155/2016/9875298.
27. Fakhari A, Gharepapagh E, Dabiri S, Gilani N. Correlation of cancer antigen 15-3 (CA15-3) serum level and bony metastases in breast cancer patients. Med J Islam Repub Iran. 2019;33:142. doi: 10.34171/mjiri.33.142.
28. Fejzić H, Mujagić S, Azabagić S, Burina M. Tumor marker CA 15-3 in breast cancer patients. Acta Med Acad. 2015;44(1):39-46. doi: 10.5644/ama2006-124.125.
29. Subramaniam D, Thombre R, Dhar A, Anant S. DNA methyltransferases: a novel target for prevention and therapy. Front Oncol. 2014;4:80. doi: 10.3389/fonc.2014.00080.
30. Miremadi A, Oestergaard MZ, Pharoah PD, Caldas C. Cancer genetics of epigenetic genes. Hum Mol Genet. 2007;16 Spec No 1:R28-49. doi: 10.1093/hmg/ddm021.
31. Ferguson-Smith AC, Greally JM. Epigenetics: perceptive enzymes. Nature. 2007;449(7159):148-9. doi: 10.1038/449148a.
32. Daina A, Michielin O, Zoete V. SwissADME: a free web tool to evaluate pharmacokinetics, drug-likeness and medicinal chemistry friendliness of small molecules. Sci Rep. 2017;7:42717. doi: 10.1038/srep42717.
33. Lipinski CA, Lombardo F, Dominy BW, Feeney PJ. Experimental and computational approaches to estimate

solubility and permeability in drug discovery and development settings. Adv Drug Deliv Rev. 2012;64 Suppl:4-17. doi: 10.1016/j.addr.2012.09.019.
34. Alturki NA, Mashraqi MM, Alzamami A, Alghamdi YS, Alharthi AA, Asiri SA, et al. In-silico screening and molecular dynamics simulation of drug bank experimental compounds against SARS-CoV-2. Molecules. 2022;27(14):4391. doi: 10.3390/molecules27144391.
35. Balogun TA, Iqbal MN, Saibu OA, Akintubosun MO, Lateef OM, Nneka UC, et al. Discovery of potential HER2 inhibitors from *Mangifera indica* for the treatment of HER2-positive breast cancer: an integrated computational approach. J Biomol Struct Dyn. 2022;40(23):12772-84. doi: 10.1080/07391102.2021.1975570.
36. Johnson TO, Adegboyega AE, Ojo OA, Yusuf AJ, Iwaloye O, Ugwah-Oguejiofor CJ, et al. A computational approach to elucidate the interactions of chemicals from *Artemisia annua* targeted toward SARS-CoV-2 main protease inhibition for COVID-19 treatment. Front Med (Lausanne). 2022;9:907583. doi: 10.3389/fmed.2022.907583.